Biomaterials Science

ROYAL SOCIETY OF CHEMISTRY

PAPER

View Article Online
View Journal | View Issue

Cite this: *Biomater. Sci.*, 2024, **12**, 151

A thermosensitive hydrogel formulation of phage and colistin combination for the management of multidrug-resistant *Acinetobacter baumannii* wound infections

Subhankar Mukhopadhyay,[a] Kenneth K. W. To,[a] Yannan Liu,[b] Changqing Bai[c] and Sharon S. Y. Leung *[a]

Chronic skin wounds are often associated with multidrug-resistant bacteria, impeding the healing process. Bacteriophage (phage) therapy has been revitalized as a promising strategy to counter the growing concerns of antibiotic resistance. However, phage monotherapy also faces several application drawbacks, such as a narrow host spectrum, the advent of resistant phenotypes and poor stability of phage preparations. Phage–antibiotic synergistic (PAS) combination therapy has recently been suggested as a possible approach to overcome these shortcomings. In the present study, we employed a model PAS combination containing a vB_AbaM-IME-AB2 phage and colistin to develop stable wound dressings of PAS to mitigate infections associated with *Acinetobacter baumannii*. A set of thermosensitive hydrogels were synthesized with varying amounts of Pluronic® F-127 (PF-127 at 15, 17.5 and 20 w/w%) modified with/without 3 w/w% hydroxypropyl methylcellulose (HPMC). Most hydrogel formulations had a gelation temperature around skin temperature, suitable for topical application. The solidified gels were capable of releasing the encapsulated phage and colistin in a sustained manner to kill bacteria. The highest bactericidal effect was achieved with the formulation containing 17.5% PF-127 and 3% HPMC (F5), which effectively killed bacteria in both planktonic (by 5.66 log) and biofilm (by 3 log) states and inhibited bacterial regrowth. Good storage stability of F5 was also noted with negligible activity loss after 9 months of storage at 4 °C. The *ex vivo* antibacterial efficacy of the F5 hydrogel formulation was also investigated in a pork skin wound infection model, where it significantly reduced the bacterial burden by 4.65 log. These positive outcomes warrant its further development as a topical PAS-wound dressing.

Received 24th August 2023,
Accepted 16th October 2023

DOI: 10.1039/d3bm01383a

rsc.li/biomaterials-science

Introduction

Skin is the largest organ of the body and acts as a first line of defense against external pathogens.[1] After a skin injury, the natural healing process can be impeded by opportunistic bacteria, potentially leading to prolonged wound healing and an increased risk of severe infection.[2,3] The complex nature of chronic wound infections, including biofilm formation,[4] antibiotic resistance[5] and hypoxia,[6] contributes to the limited efficacy of many antibiotics and promotes bacterial persistence. Skin and soft tissue infections (SSTIs) are mostly caused by *Escherichia coli*,[7] methicillin-resistant *Staphylococcus aureus* (MRSA)[7,8] and *Pseudomonas aeruginosa*.[9] However, the rapid emergence of multidrug-resistant (MDR) *Acinetobacter baumannii* and the lack of effective antibiotics pose significant medical challenges to their associated SSTIs.[10,11] Also, *A. baumannii* traumatic wound infections have drawn significant attention due to an increase in epidemics among combat injury and natural catastrophe victims.[12] In Iraq and Afghanistan, highly resistant *A. baumannii* strains are common and frequently cause fatal wound infections.[13,14] Outbreaks of pan- and MDR-resistant *A. baumannii* have raised concerns in both military and non-military scenarios. Finding alternative antibacterial strategies is, therefore, essential.

Recently, bacteriophage (phage) therapy has been adopted as a renewed strategy to combat infections caused by MDR bacteria.[15,16] However, phage monotherapy likely fails to evolve into a robust antimicrobial treatment due to a number of drawbacks, chief among which is the generation of phage-resistant phenotypes (*i.e.* bacteria develop resistance to phages) through mutation or acquisition of phage-resistant

[a]*School of Pharmacy, Faculty of Medicine, The Chinese University of Hong Kong, Shatin, New Territories, Hong Kong. E-mail: sharon.leung@cuhk.edu.hk*
[b]*Emergency Medicine Clinical Research Center, Beijing Chao-Yang Hospital, Capital Medical University, Beijing, 100020, China*
[c]*Department of Respiratory Medicine, Shenzhen University General Hospital, Shenzhen University Clinical Medical Academy, Guangdong, 518055, China*

genes.[17,18] In addition, the narrow host range of phages results in limitations to their application range or no/ineffective bacterial killing against non-specific bacteria.[19] Moreover, the pharmacokinetics of phages, including their stability and clearance from the body, can affect their therapeutic efficacy.[20] These combined factors contribute to the challenges and potential shortcomings of phage monotherapy. On the other hand, concomitant applications of phages and antibiotics have been proven to be more effective in killing bacteria and suppressing the evolution of resistant phenotypes compared to monotherapies.[21,22]

The stability of phage preparations and effective delivery to the wound site are crucial for successful phage therapy, highlighting the dual challenge of designing a topical formulation for the co-delivery of phage and antibiotic combinations to achieve positive treatment outcomes.[23,24] First, the formulation should maintain the stability of both antibacterial agents upon storage and application. Also, it should be capable of retaining the medications at the wound site for a sufficiently long time to achieve an effective treatment.

Hydrogels, three-dimensional (3D) networks of hydrophilic polymers, have been widely employed in pharmaceutical and medicinal industries for decades.[25] They have also attracted significant interest in the effective delivery of phages to manage wound,[26,27] bone and joint implant[28,29] infections. The development of antibiotic-loaded hydrogels has also received significant attention.[30] *In vivo* evaluations using rat models demonstrated that "smart hydrogels" exhibited excellent wound closure effectiveness and post-wound-closure care. These results indicated the significant potential of hydrogels for treating skin incisions and infected skin wounds.[31] To date, investigations into hydrogel-based PAS formulations for topical administration are rather limited. Among the few studies, the use of phage MR10 and minocycline in a binary hydrogel made of polyvinyl alcohol (PVA) and sodium alginate (SA) dramatically reduced MRSA-induced burn wound infection in mice.[32] Another study showed that the combination of the phage PEV20 and ciprofloxacin encapsulated wound dressing of sodium alginate–carboxymethyl cellulose (SA–CMC) synergistically killed (~95%) *P. aeruginosa in vitro*.[9] While these pre-formed hydrogels demonstrated good potential for the delivery of PAS combination, *in situ* hydrogels are more favorable as they cause minimum tissue damage upon application and can keep the wound environment wet to facilitate wound healing.[33,34]

Various polymers exhibiting thermoresponsive behavior have been popular wound dressing materials. Pluronic® F-127 (also known as PF-127 or Poloxamer 407), a non-ionic triblock copolymer composed of poly(ethylene oxide)$_{100}$–poly(propylene oxide)$_{65}$–poly(ethylene oxide)$_{100}$ (PEO_{100}–PPO_{65}–PEO_{100}), is one of the most studied thermosensitive gelling agents.[35] The excellent capability of PF-127 hydrogel solutions in stabilizing phages has also been recently reported,[27] showing great potential as the delivery vehicle for phages. However, the mechanical strength and bioadhesiveness of sole PF-127 hydrogel are relatively weak, limiting its performance as a drug delivery system. Bioadhesive polymers, such as carbomers, hyaluronic acid, chitosan and cellulose derivatives such as sodium carboxymethylcellulose and hydroxypropyl methylcellulose (HPMC), are often blended/grafted with PF-127 to improve the gel strength and bioadhesiveness.[36–38]

In the present study, we evaluated the suitability of a binary system of PF-127 and HMPC in delivering PAS combinations for wound infection management. Previously, we have identified that the phage vB_AbaM-IME-AB2 (IME-AB2 in short) and colistin combination exhibited superior antibacterial activity and was refractory to resistance development upon simultaneous application.[39] We synthesized multiple PAS hydrogel solutions with different amounts of PF-127 (15–20 wt%), modifying with/without 3 wt% of HPMC. The optimized PAS-loaded formulation was identified based on the gelation temperature and the antibacterial activity *in vitro*. The clinical potential of the optimized formulation was evaluated with an *ex vivo* porcine skin wound infection model. Our study is among the first to develop stable thermosensitive wound dressings for the co-delivery of phages and antibiotics to achieve PAS bacterial killing. The promising findings of this simple wound dressing warrant further *in vivo* investigation to translate it to clinical settings.

Materials and methods

Materials

A lytic *A. baumannii* phage IME-AB2 (*Myoviridae*) and the host bacteria MDR-AB2 were gifted from the Beijing Institute of Microbiology and Epidemiology.[40] A purified phage suspension was achieved by anion exchange chromatography using a CIMmultus™ QA 1 mL Monolithic Column (BIA Separations, Slovenia).[41] Phosphate buffered saline (PBS, pH 7.4) was used to dialyze the phage elution to give a phage stock with a titer of 1.6×10^{10} plaque-forming units (PFU) mL^{-1}. Colistin was purchased from J&K Scientific (Beijing, China) (cat. no. 437689, >19 000 IU mg^{-1}). PF-127, HPMC, PBS and paraformaldehyde (PFA) were purchased from Sigma-Aldrich (St Louis, MO, USA). Nutrient broth (NB) and bacteriological agar (Agar No. 1) were supplied by Oxoid (Hampshire, UK). Ethanol (99.8%) was procured from Thermo Fisher Scientific (Loughborough, UK). Fresh Milli-Q water was dispensed from a Milli-Q Integral water purification system (Burlington, MA, USA) with a resistivity of 18.2 MΩ cm at 25 °C.

Preparation of the phage–antibiotic incorporated thermoresponsive hydrogel

The concentrations of PF-127 (15–20%) and HPMC (3%) were selected based on a previous research study,[36] in which the hydrogel combinations showed a thermoresponsive behavior with gelation temperatures close to the human skin temperature 33.5–36.9 °C.[42] Briefly, HPMC powder was first fully dissolved in Milli-Q water at 60 °C with magnetic stirring, followed by the addition of PF-127 at different w/w% ratios as detailed in Table 1. For the pure PF-127 gel solution, it was

Table 1 Compositions and gelling temperature of different hydrogel formulations

Formulations	PF-127 (wt%)	HPMC (wt%)	$T_{sol-gel}$ (°C)	Gelling time at 34 °C (seconds)
F1	15	0	44.5	—
F2	17.5	0	33.0	24
F3	20	0	30.5	16
F4	15	3	33.5	13
F5	17.5	3	29.0	7
F6	20	3	23.0	4

prepared at room temperature with magnetic stirring as it was easily dissolved in Milli-Q water. The polymer mixtures were stored at 4 °C for two days to achieve full hydration. PBS (as blank gel), the IME-AB2 phage, colistin and their combination were then incorporated into the hydrogel solutions at a 1 : 9 v/v ratio to achieve the final phage and colistin concentrations of 10^9 PFU mL^{-1} and 80 μg mL^{-1}, respectively. The drug-loaded hydrogel was kept at 4 °C with gentle agitation for another 12 h before characterization.

Measuring the solution–gel transition temperature ($T_{sol-gel}$) and gelling time

The gelling temperature of the PAS-loaded hydrogel solutions ($T_{sol-gel}$) was determined using the tilt method as previously described.[43] Briefly, a glass vial holding 1 mL of hydrogel solution was placed in a preset temperature water bath for ~30 s. Then, the glass vial was removed from the water bath, followed by tilting to ensure the gelation of the hydrogel solution. The temperature of the water bath was increased by 0.5 °C from 20 °C until $T_{sol-gel}$ was reached (Table 1). The gelation time for all formulations at 34 °C were also recorded.

Storage stability of the PAS-loaded hydrogel solution

The stability of the phage IME-AB2 in the hydrogel solutions after storing at 4 °C for the specific time was determined by a plaque assay. In short, 20 μL of PAS-loaded hydrogel solution was mixed with 180 μL of PBS, followed by serial dilutions, and the mixture was dropped onto a bacterial agar lawn. Then, the agar plates were placed in an incubator at 37 °C overnight. The phage titer was determined by counting the plaque forming units (PFU). The antibacterial activity of the PAS-loaded hydrogel F5 was also evaluated after 9 months of storage.

Scanning electron microscopy (SEM)

The morphology of the F5 hydrogel was visualized by scanning electron microscopy (SEM), as per the previously described method.[27] At first, the liquid hydrogel solution was incubated at 37 °C to solidify. The solidified gel was then rapidly frozen using liquid nitrogen to preserve its structure, and subjected to lyophilization for three days to remove all the trapped water. The freeze-dried gel was sectioned with a scalpel and affixed to SEM metal stubs using double-sided adhesive carbon tape prior to platinum coating. Finally, the sample was visualized using a Quanta 400F SEM (FEI, Oregon, USA).

Swelling and degradation study of the hydrogel

Swelling and degradation of the PAS-loaded hydrogel were determined as per the earlier mentioned protocol.[27] Initially, 100 μL of PAS-loaded hydrogel solution was added into a cuvette and gelled by placing it inside an incubator at 37 °C for 15 min. Then, 900 μL of PBS was added to the solidified hydrogel at 37 °C with gentle shaking. The initial weight of the hydrogel (W_0) was taken. At different time intervals, PBS was withdrawn and the weight of the gel was recorded (W_t), followed by replacement with fresh PBS warmed at 37 °C. The equation to determine the swelling and degradation of the hydrogel at different time points (S_t) is given below.

$$\%\, S_t = \frac{(W_t - W_0)}{W_0} \times 100$$

In vitro release of the phage (IME-AB2) and colistin from the hydrogel

To monitor the release profile of phage and colistin from the hydrogel, 100 μL of the PAS-loaded hydrogel was placed into a microtube. It was then placed into an incubator for 15 min at 37 °C to allow gel formation. PBS solution was considered as release media and added into the tube at a 1 : 9 (gel : PBS) v/v ratio. It was then placed back into the incubator at 37 °C with mild shaking (100 rpm). At different time intervals (0, 0.16, 0.50, 2, 4, 6, 8, 24 and 48 h), 20 μL of solution was pipetted out for the plaque assay. In the colistin release study, 50 μL of sample was withdrawn at every time points (0, 2, 4, 6, 8, 24 and 48 h) for quantification of colistin by HPLC. After sample withdrawal, the same amount of fresh PBS warmed at 37 °C was added to the reaction tubes. The HPLC method for colistin measurement was modified from ref. 44. Briefly, reversed-phase chromatography was performed with a C18 column (Zorbax SB-C18, 5 μm, 4.6 × 250 mm, Agilent). The mobile phase consisted of 0.1% trifluoroacetic acid (TFA) in Milli-Q water (A) and 0.1% TFA in acetonitrile (B). The flow rate was 1 mL min^{-1} with gradient elution: 20% B to 50% B in 10 min. The injection volume was 20 μL and a DAD detector at 214 nm was used for colistin detection. A standard curve (10–50 μg mL^{-1}, $R^2 > 0.999$) was prepared for the calculation of colistin concentration.

Time–kill kinetics assay

A time–kill assay was performed to monitor the killing kinetics of hydrogels loaded with PBS (blank), phage (10^9 PFU mL^{-1}), colistin (80 μg mL^{-1}) and the combination. Briefly, 100 μL of hydrogel solution was added into a cuvette, followed by incubation at 37 °C for 15 min gel formation. Then, 900 μL of overnight cultured *A. baumannii* (OD_{600} = 1) was added to each cuvette and incubated again at 37 °C with gentle shaking (150 rpm) for up to 48 h. At pre-determined time intervals (0, 2, 4, 8, 24 and 48 h), bacterial colony counts in the NB-agar plate were quantified to determine the bactericidal effects of the

hydrogels. Phage replication upon the treatment time was also evaluated by the double-layered agar plate method.

In vitro biofilm eradication study of the PAS encapsulated hydrogel

This experiment was conducted using the previously reported method with minor modifications.[27] Briefly, fresh NB was added to overnight cultured *A. baumannii* with a final OD_{600} of ~0.2. Then, a biofilm was established in a 96-well plate by adding 100 μL of diluted bacteria in each well for incubation at 37 °C with gentle shaking (100 rpm) for 48 h. Bacterial suspensions were removed after biofilm formation, and wells were rinsed with fresh PBS twice. Next, 100 μL of samples (PBS, blank gel, phage suspension, phage gel, colistin solution, colistin gel, PAS suspension and PAS gel) were introduced into the wells, followed by 48 h incubation at 37 °C and 100 rpm shaking. After treatment, samples were placed in a refrigerator at 4 °C to liquefy the gels which were then pipetted out and wells were rinsed twice with PBS. Crystal violet (CV) staining was then performed by adding 200 μL of 0.1% (w/v) CV to each well. After 1 h of incubation at room temperature in the dark, the solution was discarded and washed thrice with PBS. Then, 200 μL of 70% ethanol was added to the wells to dissolve the retained CV with vigorous pipetting. An amount of 150 μL of the sample was transferred to a new 96-well plate for biofilm biomass quantification by OD measurements at 570 nm using a microplate reader. Bacterial counting was also conducted to evaluate the number of viable bacteria in the treated biofilms. Moreover, architectures of the treated biofilms were imaged using a fluorescence microscope (Nikon, TI-DH, Japan) after staining with the LIVE/DEAD™ BacLight™ Bacterial Viability Kit (Thermo Fisher Scientific, Massachusetts, USA). For image processing, NIS-Elements imaging software (version 5.01) was used. All experiments were performed with three biological replications in two separate experiments.

Ex vivo studies in the porcine skin wound infection model

Gel compression study. The porcine skin wound model was developed as previously described.[27] Pork skin was purchased from a local market (Fusion Plaza Ascot, Fotan, Hong Kong), cleaned with Milli-Q water, and shaved to remove hairs from the epidermal layer. It was then wrapped in plastic and preserved at −20 °C before use. To ensure sterility, defrosted skin was sliced into the desired number of pieces, and rinsed with alcohol (70%), followed by Milli-Q water. Autoclaved tissue papers were used to dry the skin surface. Then, plates with closed lids were used to store the skin. Approximately 4 mm deep and 4 mm diameter skin incisions were created by punch biopsies. The wounds were washed once again following the mentioned cleaning procedures. Next, a CV dye was mixed with the PAS-loaded gel for better visualization and administered into the wound sites, followed by incubation at 37 °C for 15 min to allow gel formation. After that, various stressors were applied, including stretching, bending, twisting and compression, to validate the robustness of gel attachment to the wound site.

Gel antibacterial assay. The above porcine skin wound model was used for the evaluation of the *ex vivo* antibacterial effectiveness of the optimized hydrogel formulation (F5). Bacterial infection was first induced by inoculating 50 μL of *A. baumannii* (OD_{600} = 0.6) into the wound site for 2 h at 37 °C. Next, an *ex vivo* antibacterial assay was performed by administering 50 μL of the control (blank gel) and treatment samples including phage-gel, colistin-gel and PAS-gel to the wound, followed by further incubation at 37 °C for 6 h. Then, plates were placed inside a refrigerator at 4 °C to transform the rigid gels into a solution form. Finally, the samples were carefully removed, PBS was added and sterile plastic loops were used to gently scratch the incision in order to collect the bacteria. The presence of viable bacteria following various treatments was quantified by NB-agar plating.

Porcine skin histological study. To visualize the skin injury, infection development by MDR-AB2 and efficacy of the PAS-combination treatment, tissue sectioning followed by hematoxylin and eosin (H&E) staining was performed. Pork skin without wound was included for comparison with the punctured skin. Wounded skins after blank and PAS-gel treatments along with normal skin were immersed for 48 h in 4% PFA for tissue fixation. The skin was then embedded in liquid paraffin for sectioning and mounted in glass slides. The sectioned tissues were then stained with H&E by following the previously described method.[45] Then, slides were washed with water, followed by dehydration with a series of different alcohol concentrations. Finally, the slides were mounted and covered with a glass coverslip for microscopic evaluations.

Statistical analysis

Unless specified, all experiments were performed with three replicates and repeated two independent times. The experimental results are represented as means ± S.D., n = 3, if not mentioned differently. The statistical significance ($P \leq 0.05$) was calculated by one-way analysis of variance (ANOVA), followed by Tukey's multiple comparison tests. GraphPad Prism software version 9.0 was used to generate all the graphs and perform the statistical analysis.

Results and discussion

Influence of HPMC on $T_{sol-gel}$

As illustrated in Fig. 1A, thermosensitive PF-127 was employed as the major gelation agent and 3% HMPC was added to the hydrogel systems to improve the overall gel strength and bioadhesiveness.[36]

An ideal thermosensitive hydrogel wound dressing should remain as a solution at the ambient temperature and have a $T_{sol-gel}$ slightly below the skin temperature in the range of 33.5–36.9 °C.[42] In this way, the flowing hydrogel solution can fill the wound bed and subsequently form a semi-solid gel in the shape of the wound bed. Fig. 1B shows that the flowable hydrogel solution changes to a rigid gel at $T_{sol-gel}$. According to Table 1, the $T_{sol-gel}$ of prepared PAS-loaded hydrogel formu-

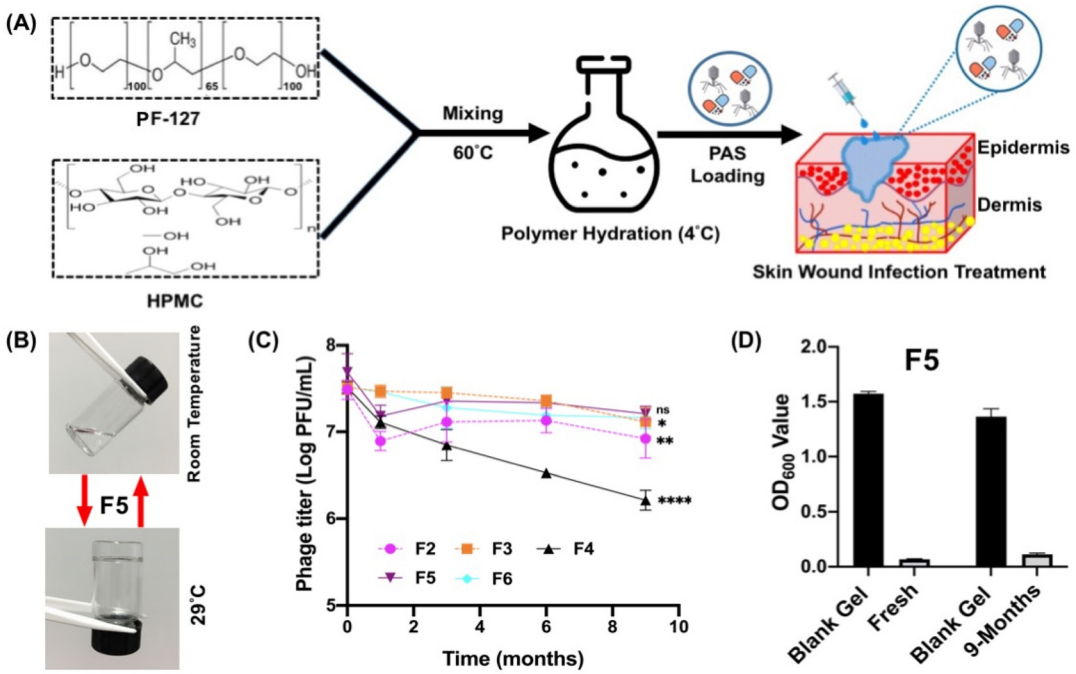

Fig. 1 (A) Scheme of the synthesis and intended application of the PAS-embedded HPMC:PF-127 hydrogel. (B) Thermogel solution (F5) at room temperature (free flowing solution) and 29 °C (solid gel matrix). Monitoring the (C) stability and titer loss of the phage IME-AB2 at 9 months after being stored in a series of hydrogel formulations (F2–F6) at 4 °C. (D) Overall bacteria killing ability of fresh PAS gel (F5) and after 9-months of storage at 4 °C. All values are expressed as means ± S.D., n = 3. Significant differences are indicated by asterisks (*$P \leq 0.05$, **$P \leq 0.01$, ****$P \leq 0.0001$) and ns = no significant difference ($P > 0.05$) from the initial phage titer.

lations were close to the human skin temperature, except F1 (containing 15% PF-127) with a $T_{sol-gel}$ of 44.5 °C. It was noticed that the addition of HMPC significantly lowered the $T_{sol-gel}$ of PF-127 hydrogel solutions by at least 4 °C. In addition, it was also observed that the inclusion of HPMC speeded up the gelation process (at 34 °C) of the binary systems by reducing the gelation time (Table 1).

Previous studies revealed that the presence of HPMC enhanced the viscosity of the hydrogel system and reduced the critical micelle concentration of PF-127.[46,47] It was reported that the interaction of these two polymers resulted in the formation of hydrogen bonds between the cellulose derivative and the PEO blocks of PF-127. These hydrogen bonds may cause a reduction in the effective block length of PEO, ultimately promoting micellization and thereby influencing the gelation temperature.[48] The favorable interaction of HPMC with water might also reduce the amount of water available to hydrate the poloxamer chains.[36] These phenomena could contribute to the lower gelation temperature in the binary polymeric mixture and the shorter gelation time required. As the $T_{sol-gel}$ of F1 fell outside the desirable range, this formulation was discarded for further study.

Storage stability of PAS-loaded hydrogel solutions

The viability of phages in the remaining five hydrogel solutions (F2–F6) after storing at 4 °C for a certain period was examined. The stability data in Fig. 1C show that F4 (containing 15% PF-127 and 3% HMPC) had the greatest phage loss after 9 months of storage, ~1.3 log PFU mL^{-1} loss compared with the titer detected in the freshly prepared hydrogel solution. On the other hand, the other four hydrogel solutions could effectively stabilize the incorporated IME-AB2 phage, that only up to ~0.5 log PFU mL^{-1} loss was noted after 9 months of storage.

Recently, Yan *et al.* reported the excellent stability of the IME-AB2 phage in 18 wt% PF-127 solution that negligible titer loss was noted after 24 months of storage at 4 °C.[27] They suggested that the non-ionic triblock copolymer PF-127 could stabilize the phage by creating hydrogen bonding with the phage and offering steric hindrance to reduce phage aggregation.[27] Good short-term storage stability and significant antibacterial efficacy were also reported for colistin-crosslinked PF-127 micelles.[49] HPMC was reported to be an applicable delivery vehicle for various phages. Chang *et al.* reported negligible phage-titer loss (~0.4–0.5 log) for the phage PEV1 and PEV31 in 5% HPMC gel after being stored for 8 weeks at 4 °C.[50] Similar findings were reported for the phage Kpn5 stored in 3% HPMC hydrogel at 37 °C over a period of 1 week.[51] However, one study raised concern over the phage stability in the HPMC gel, that a ~3 log PFU mL^{-1} titer reduction was detected for the phage MR-5 in 4% (w/v) HPMC gel after 20 days of storage.[52] Hence, phage-specific stability in HPMC may exist. Therefore, phage–HPMC interactions in the

hydrogel solution with a higher HPMC to PF-127 ratio (3 : 15 w/w%) could be a possible reason for the higher titer loss for F4 when compared with the other two HPMC containing formulations, F5 and F6.

Next, the bacteria killing ability of the stored PAS-loaded gel was verified. The bacteria killing data (Fig. 1D) confirmed the potential antibacterial efficiency of the fresh PAS-loaded F5 hydrogel. In addition, it ensured that the combination of two polymers did not reduce the effectiveness of the phage–colistin combination and retained their viability for at least 9 months.

Antibacterial activity of the PAS-loaded hydrogels

Due to the lower storage stability of F4, it was not included for the antibacterial assessments. Fig. 2 shows the antibacterial efficiencies of the four PAS hydrogel formulations which demonstrated superior phage storage stability (F2, F3, F5 and F6). All PAS-loaded hydrogels exhibited significant bacterial reduction (>3 log colony-forming units (CFU) per mL), similar to the suspension form, suggesting that the encapsulated phage and colistin could be released from the hydrogel networks to exert their bacterial killing effects.

Formulations containing PF-127-only (F2 and F3) showed a higher bactericidal effect than those modified with 3% HMPC (F5 and F6) in the first 8 h, but both formulations failed to suppress bacterial regrowth after 48 h of treatment. On the other hand, the two binary hydrogel systems (F5 and F6) demonstrated better suppression of bacterial regrowth over the whole observation period, though the antibacterial effect was slightly delayed. Comparing the two binary systems, F5 exhibited a higher *in vitro* antibacterial effect, that it drastically reduced the bacterial burden by 5.66 log. Containing a higher amount of PF-127 content (20%), F6 started with a lower level of bacterial killing potency and maintained a consistent ~3 log reduction in the bacterial population with only a slight regrowth after 48 h of treatment.

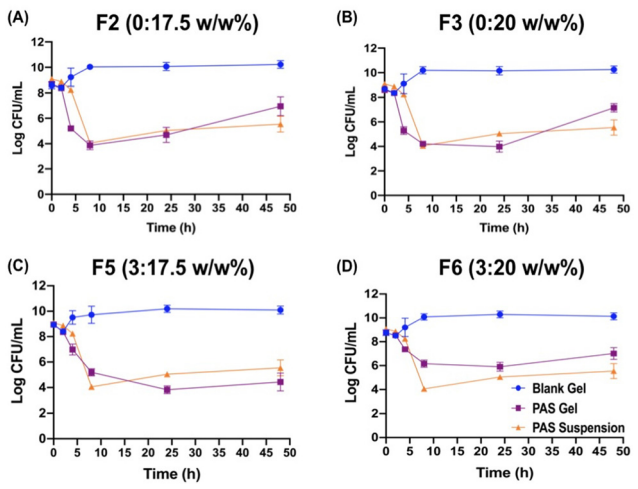

Fig. 2 *In vitro* time–kill kinetics (TKA) of the PAS-loaded hydrogel formulations (HPMC : PF-127): (A) F2, (B) F3, (C) F5 and (D) F6 along with the PAS combination suspension against MDR-AB2. All values are expressed as means ± S.D., n = 3.

The efficient bacterial killing with PAS-loaded hydrogels was also reported in previous studies. The phage MR10 and minocycline-loaded PVA–SA hydrogel wound dressing effectively reduced bacteria (~2 log) from skin[32] and the PAS-combination (phage PEV20 + ciprofloxacin) encapsulated wound dressing of SA–CMC synergistically killed (~95%) *P. aeruginosa*.[9] The appropriate hydrogel compositions (F5) could not only retain the excellent bactericidal effect of the PAS combination, but also facilitated the suppression of resistance emergence. Chronic wound infections are usually associated with negative antibiotic treatment outcomes due to the formation of robust biofilms and emergence of antibiotic-resistant bacteria.[53,54] Effective bacterial load reduction plays a crucial role in reducing the infection burden, thereby decreasing the risk of persistent inflammation, delayed wound healing and systemic spread of infection. By lowering the bacterial load, the immune system can also more effectively combat the infection and prioritize wound repair.[55] In other words, maximizing bacterial reduction in wound areas is essential in facilitating optimal healing and minimizing the potential complications associated with these infections. In this regard, F5 exhibiting the best killing efficiency (Fig. 2C) was chosen for detailed characterization.

In vitro physiochemical characterization

Swelling and degradation profile. The *in vitro* swelling and degradation profile of the PAS-loaded F5 hydrogel is depicted in Fig. 3A. The gel absorbed the swelling media (PBS, pH 7.4) with a slow increase in the swelling ratio for up to 8 h (~43%). After that, the moisture uptake rate drastically increased to reach its maximum swelling ratio (90%) at 12 h. Then, the gel started to degrade gradually and reached ~100% gel degradation in 2 days.

As previous studies reported, the hydrogel composed of PF-127 alone has shown rapid swelling and erosion.[27,56] With the addition of the hydrophilic polymers, such as carrageenan, xanthan gum, and HPMC, the degradation rates of hydrogels were significantly delayed.[56] It is hypothesized that, for F5, the introduction of HPMC into the PF-127 gel network results in an increased number of cross-links between PF-127 micelles.[57] As a result, there was a greater level of entanglement and stiffness of the gel structure. This leads to a longer duration for the hydration and dissolution of the polymer chains, which further slows down the gel erosion.

Morphology of the hydrogel. As shown in Fig. 3B, the optimized hydrogel F5 displayed a well-defined round and oval shaped porous morphology with a lamellar arrangement. This result was in good agreement with a previous report.[46] The hydrophobic core of the micelles can interact with the cellulose derivatives through hydrogen bonding and other interactions when micellar copolymers and cellulose derivatives are mixed in a formulation.[58] These interactions resulted in the development of a network structure, which may alter the mor-

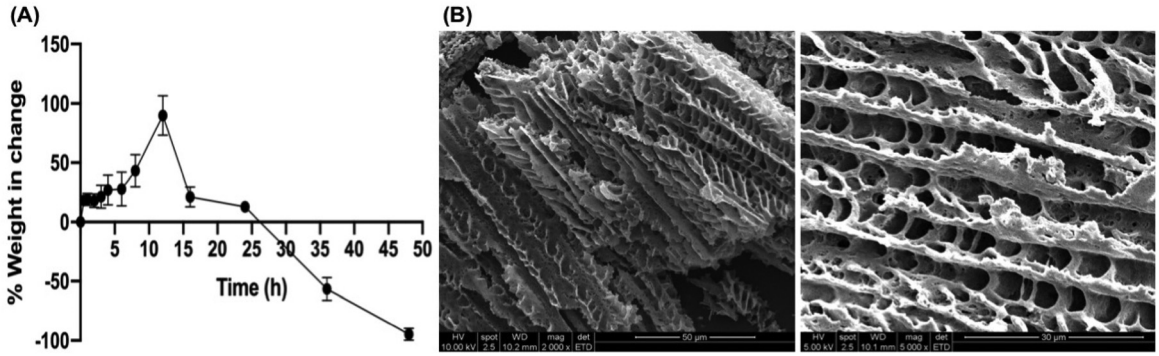

Fig. 3 (A) Swelling and degradation profile of F5 at 37 °C. All values are expressed as means ± S.D., n = 3. (B) SEM images of the F5 hydrogel at ×2000 (scale bar: 50 μm) and ×5000 (scale bar: 30 μm) magnifications.

phological framework of the formulation and micelle dimensions for the cellulose derivative.[46]

Prior cross-sectional SEM images of the thermosensitive hydrogel with PF-127 indicated a compact, perplexing, tube-like structure with improved porosity,[27,59] which often corresponds to improved permeability and solubility. The porous structures would facilitate the release of incorporated antimicrobials by degrading the hydrogel matrix when exposed to the release media.

In vitro release profile of the phage IME-AB2 and colistin

The release of phage and colistin from the selected hydrogel (F5) is depicted in Fig. 4A. F5 sustained the release of both antimicrobials for up to 48 h. Initially, a release of ~5.4 log PFU phage titer (~2%) was detected in the medium upon the addition of the release media. Later at 24 h, 75.06% phage release (~7.13 log PFU) was noticed. Although there was no colistin release detected for the first 2 h, colistin release eventually followed a similar pattern to that of the phage. Sustained releases of colistin from the hydrogel matrix continued with a higher cumulative release of colistin noted at 24 h (~95% release) and 100% colistin release was achieved at 48 h of incubation. The immediately released phage, even at a low level, could facilitate the initial phase of bacteria killing (in the first 2 h) and synergized with the subsequently released colistin, leading to a significant reduction in the bacterial density (Fig. 2C). This was in accordance with our previous findings that both phage first and simultaneous PAS treatment yielded superior synergistic bacterial killing than the antibiotic first treatment.[39]

Fig. 4B depicts that the sustained release of colistin from the combination gel had no significant impact on phage replication, which was comparable with that of the phage-only gel. The low amount of colistin released at the intial stage could be the reason, because the presence of a higher antibiotic concentration at the beginning could negatively impact the phage replication process.[60,61] PAS combination gel, along with the phage-only gel, displayed a progressive increase in phage titer for up to 4 h (~10^{11} PFU mL^{-1}), after which they both reached a plateau. The phage and colistin release profile was best fitted with the Hixson–Crowell mathematical release model with the

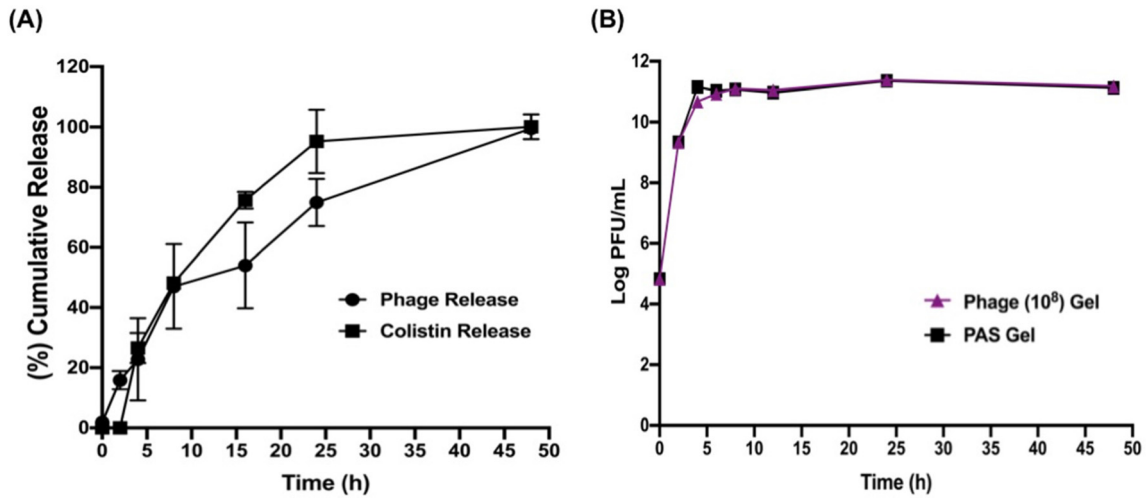

Fig. 4 (A) Percentage cumulative release profile of the phage IME-AB2 and colistin from the F5 hydrogel. (B) Influence of the only-phage gel and PAS gel on the phage propagation rate. All values are expressed as means ± S.D., n = 3.

Table 2 Parameters of various mathematical release models

	Phage IME-AB2			Colistin		
Mathematical model	R^2	Slope	Intercept	R^2	Slope	Intercept
Zero-order	0.8956	1.9249	17.086	0.7544	2.1639	17.8640
First-order	0.7122	35.311	3.2406	0.9703	−0.0444	2.0238
Higuchi	0.9821	14.741	−1.3421	0.9046	17.33	−5.2416
Korsmeyer–Peppas	0.8416	0.9039	0.6567	0.8300	1.3545	0.1059
Hixson–Crowell	0.9832	0.077	0.0055	0.9789	0.1008	0.063

highest correlation coefficient value (R^2) as shown in Table 2. This result shows that the release of these two antimicrobials mostly depend on the erosion and degradation of the hydrogel matrix over time with little impact resulted by diffusion.[62,63]

In vitro antibiofilm activity

A. baumannii possessed excellent capacity in biofilm formation, being an important virulent factor for its infections.[64] Although a few studies reported the effectiveness of the phage hydrogel in treating biofilms,[27,65,66] research into the antibiofilm ability of the PAS-loaded hydrogel is lacking. In this study, we compared the antibiofilm efficiency of the different treatment groups in both the gel and suspension/solution forms. According to Fig. 5A, no significant difference was noted between the suspension/solution and gel forms of all tested antibacterial agents, suggesting that the hydrogel had no impact on the overall bacterial killing. Among all tested agents, the highest biofilm biomass reduction was noticed for PAS combination. PBS and the blank gel showed no antibiofilm capacities (OD_{570} value of ~4). Phage and colistin monotherapies could remove biofilm biomass to some extent, but lower than that achieved by the combination treatment.

The viability of bacteria in the biofilm was also evaluated (Fig. 5B). No bacteria killing in the biofilm state was recorded after PBS and blank gel treatments. Corresponding to the biomass removal data, the PAS combination suspension and gel demonstrated the highest levels of bacterial population inhibition (3.47 log and 3 log, respectively), with no discernible variation between them. Biofilms exhibit remarkable resistance to antibiotics compared with planktonic cells. Studies provided evidence that when microorganisms form biofilms, they can become 10–1000 times more resilient against the impact of antimicrobial agents.[67] The polysaccharide biofilm matrix acts as a barrier, hindering the access of antimicrobials to the bacterial cells. The IME-AB2 phage is a depolymerase-bearing phage and the capability of the encoded depolymerase in degrading the extracellular polysaccharide substances (EPS) has been previously reported.[68] We anticipated that the IME-AB2 phage could effectively degrade the EPS within the biofilm to facilitate the penetration of colistin into the biofilm to boost the antibiofilm capacity of the PAS combination.[39] Fig. 5 confirms that the incorporation of the IME-AB2 phage and colistin combination into the hydrogel system had negligible impact on their synergy, outperforming the gels incorporated into the single agent. It is expected that PAS-loaded F5 hydrogel-mediated higher antibiofilm activity can mitigate the infections more effectively in chronic wounds to enhance wound healing.

After the various treatments, the biofilm architectures were also visualized (Fig. 5C) using a fluorescence microscope after Live/Dead™ BacLight™ staining. A green fluorescent dye SYTO 9 was used to visualize live bacteria where a red fluorescent dye propidium iodide (PI) indicated dead bacterial cells. The data were in good accordance with the crystal violet staining and bacterial viability data.

Ex vivo evaluations

A porcine skin model was employed to evaluate the applicability and therapeutic efficacy of the optimized PAS-loaded thermosensitive hydrogel (F5) *ex vivo*. When the hydrogel solution was placed on the skin wound and incubated at 34 °C, proper gelation was seen. Several mechanical forces, including stretching, bending, twisting, and compressing, were also applied, as illustrated in Fig. 6A, to demonstrate the rigidity of the formed gel on skin wounds. This further guaranteed its use as a topical wound dressing.

An antibacterial study was then performed in the pork skin wound infection model (Fig. 6B). A significant bactericidal effect was noticed for the PAS combination suspension (~5.36 log reduction) and gel (~4.65 log reduction) when compared with the controls (PBS, blank gel), and phage and antibiotic monotherapies. There was no noticeable distinction between PBS and the blank gel. Due to the immediate availability of the antibacterial agents, the solution/suspension form demonstrated a slight superior antibacterial activity over the gel form for the phage, colistin and combination treatments.

Next, histopathological evaluations were conducted to confirm the antibacterial efficacy of the PAS gel and its impacts on the skin tissues. As seen in Fig. 7A, the normal pork skin section without wound retained its structure, which includes epidermis, dermis, hair follicles, connective tissue, adipose tissue and skeletal muscle. On the other hand, the loss of epidermis can be seen in Fig. 7D, which validates the formation of wound by punch biopsies. In the case of the blank gel-treated wound infection, large numbers of MDR-AB2 were present within the epithelium of hair follicles, deeper collagen and dermal layer (Fig. 7B and C). There was also a diffuse eosinophilic homogeneous appearance to the exposed collagenous connective tissue associated with clumps of bac-

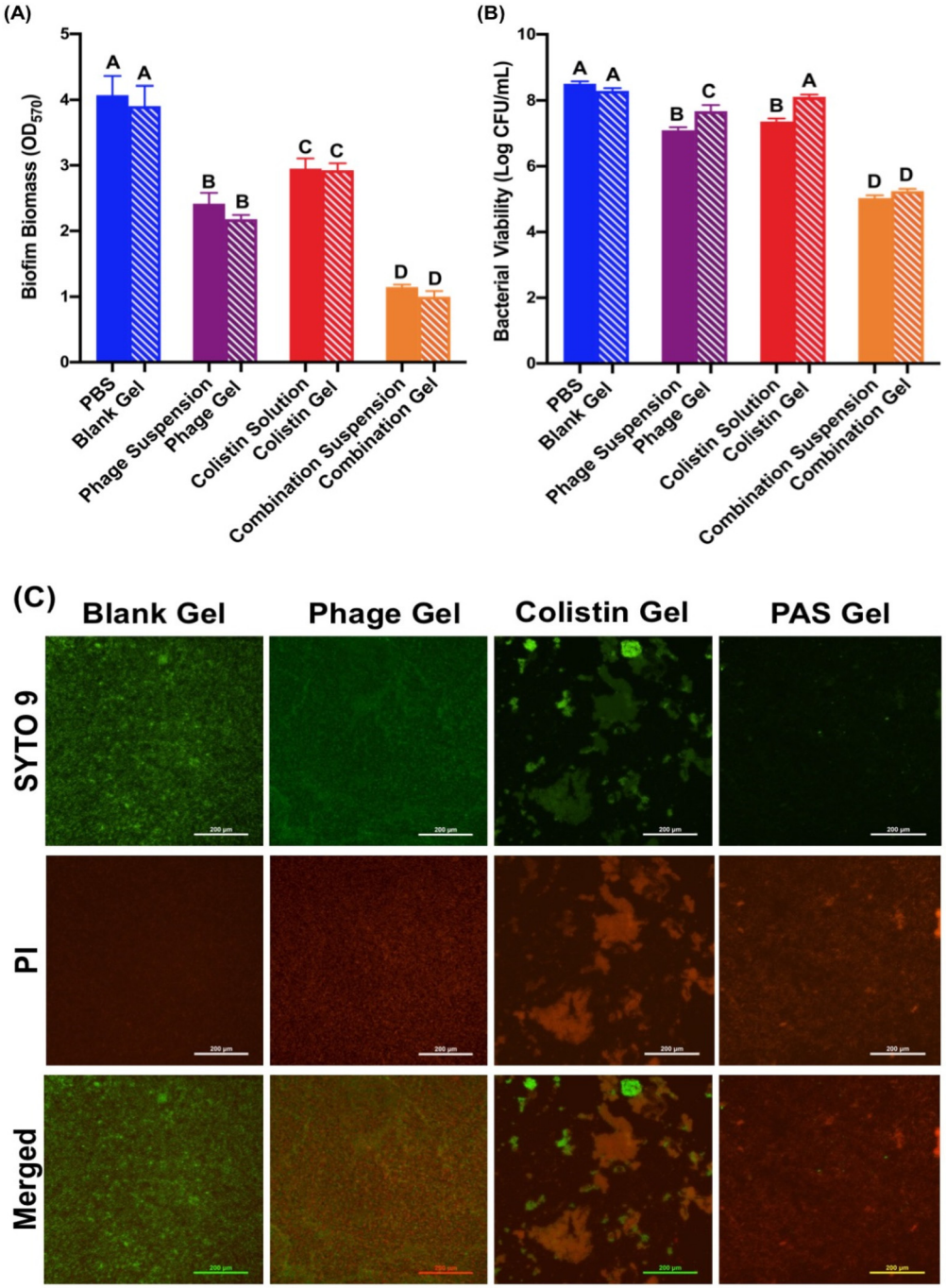

Fig. 5 *In vitro* antibiofilm activity of the controls (PBS and blank gel) and the treatments (phage, colistin and their PAS combination in the suspension/solution and gel form). (A) Biofilm biomass reduction of bacteria in the presence of the different treatment samples. (B) Quantification of viable bacteria counts in biofilms after the various treatments. Shared letters represent no significant differences ($P > 0.05$). Non-shared letters represent significant differences ($P < 0.05$). (C) Fluorescence microscopy images of the biofilm architecture after the various treatments. SYTO 9: green fluorescent nucleic acid stain for living cells, PI (propidium iodide): red-fluorescent dye for dead cell staining, Merged: merged fluorescence images of the biofilm. Scale bar: 200 μm.

teria on the surface. Differently, the PAS combination gel-treated skin section demonstrated relatively less MDR-AB2 presence among the superficial dermal collagen without inflammation (Fig. 7D). Also, the adipose tissue, connective tissue and skeletal muscle were within normal limits. This qualitative outcome was consistent with an earlier *ex vivo* study on bacterial colony counts (Fig. 6B).

The overall trend in *ex vivo* bacteria killing coincided with the earlier *in vitro* findings. The PAS combination loaded hydrogel demonstrated a synergistic antibacterial effect and

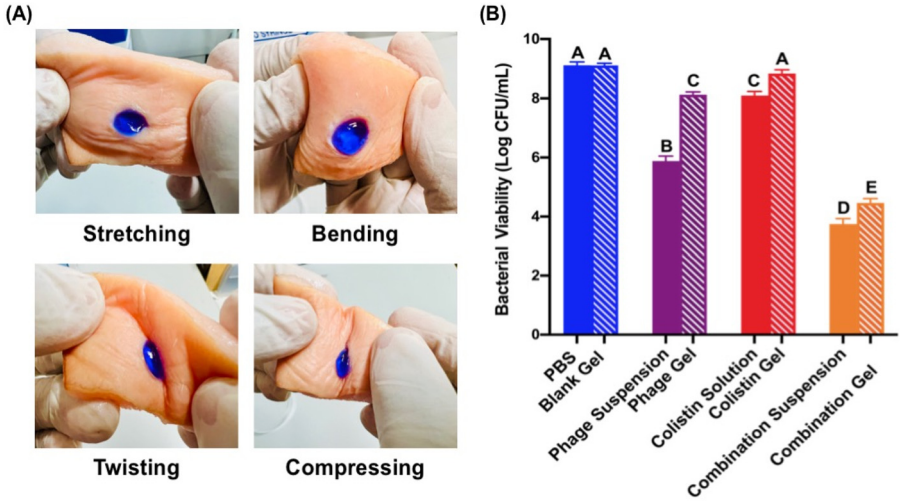

Fig. 6 (A) Images of the hydrogel after application of various mechanical stresses such as stretching, bending, twisting and compressing. (B) *Ex vivo* antibacterial efficacy of the controls (PBS and blank gel) and treatments (phage, colistin and their PAS combination in the suspension/solution and gel form). All values are expressed as means ± S.D., $n = 3$. Shared letters represent no significant differences ($P > 0.05$). Non-shared letters represent significant differences ($P < 0.05$).

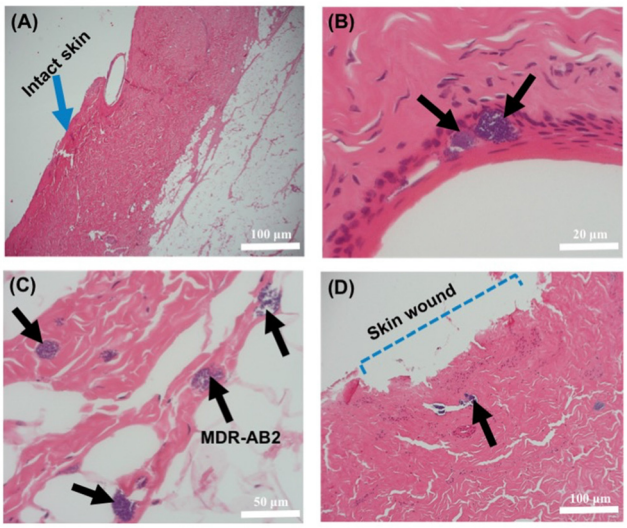

Fig. 7 Histology of (A) normal pork skin without wound and the MDR-AB2 infected wound treated with the (B and C) blank and the (D) PAS gel. Blue arrow: intact skin, black arrows: presence of bacteria and blue dash-line: skin wound.

proved to be a suitable and effective candidate to manage skin wound infection *ex vivo*, which further increases the likelihood of its potential *in vivo* application. While the binary hydrogel containing 17.5 wt% PF-127 and 3% HPMC was demonstrated to be a suitable drug delivery system for PAS combination to manage wound infection, it is important to note that the conclusion is drawn based on the findings of one specific PAS combination against one bacterial species, *A. baumannii*. To determine whether the results are extendable, additional validation is required by investigating the stability of different PAS combinations in these binary polymeric systems, as phage–polymer interactions are likely to be phage-specific.[50–52]

Conclusion

PAS has attracted increasing attention in managing MDR bacterial infection. The formulation development for effective delivery of PAS for the management of wound infections is scarce. In this study, we have developed a binary thermosensitive hydrogel wound dressing containing 17.5 wt% PF127 and 3% HPMC, which exhibited good physicochemical traits, including the formation of an *in situ* gel at skin temperature, capable of absorbing large amount of moisture and providing a controlled release of both therapeutic agents. It not only synergistically killed bacteria in both the planktonic and biofilm states, but also prevented bacteria from growing again during the course of the treatment. Importantly, the formulation could stabilize the PAS combination upon storage at 4 °C for at least 9 months. This addressed a major pitfall related to the stability of the phage products. Finally, the *ex vivo* studies reaffirmed its applicability and therapeutic potency as a topical wound dressing. Although PF-127 and HMPC have been widely included in pharmaceutical products, *ex vivo* research to reaffirm their safety is important for their intended application. The encouraging results obtained from this study also call for additional *in vivo* research to provide additional insight into their potential clinical use in combating MDR-*A. baumannii* skin wound infections.

Data availability

vB_AbaM-IME-AB2 has been deposited in the NCBI nucleotide sequence database under GenBank accession number: JX976549.

Author contributions

Conceptualization, SM, KKWT, CB and SSYL; methodology, SM and YL; data analysis, SM and YL; resources, YL and CB; supervision, KKWT and SSYL; writing – original draft preparation, SM; writing – reviewing: YL, CB, KKWT and SSYL; and funding acquisition, SSYL. All authors have read and agreed to the published version of the manuscript.

Conflicts of interest

The authors declare that they have no known competing financial interests or personal relationships that could have appeared to influence the work reported in this paper.

Acknowledgements

This work was funded by the University Grants Committee of Hong Kong (ref. 14112921). S. Mukhopadhyay is supported by the HKPFS provided by the University Grants Committee. The authors are thankful to Beijing Institute of Microbiology and Epidemiology for their kind donation of the bacterial strain MDR-AB2 and the IME-AB2 phage tested in the present study. Special thanks to Mr Andrew Li from the Department of Physics, the Chinese University of Hong Kong for the help with SEM and the CityU Veterinary Diagnostic Laboratory (CityU VDL) for the assistance with pork skin histology.

References

1 Y. Lu, M. Zhao, Y. Peng, S. He, X. Zhu, C. Hu, G. Xia, T. Zuo, X. Zhang and Y. Yun, A physicochemical double-cross-linked gelatin hydrogel with enhanced antibacterial and anti-inflammatory capabilities for improving wound healing, *J. Nanobiotechnol.*, 2022, **20**, 1–26.
2 S. L. Percival, C. Emanuel, K. F. Cutting and D. W. Williams, Microbiology of the skin and the role of biofilms in infection, *Int. Wound J.*, 2012, **9**, 14–32.
3 H. Sorg, D. J. Tilkorn, S. Hager, J. Hauser and U. Mirastschijski, Skin wound healing: an update on the current knowledge and concepts, *Eur. Surg. Res.*, 2017, **58**, 81–94.
4 K. Razdan, J. Garcia-Lara, V. Sinha and K. K. Singh, Pharmaceutical strategies for the treatment of bacterial biofilms in chronic wounds, *Drug Discovery Today*, 2022, **27**, 2137–2150.
5 E. M. Darby, E. Trampari, P. Siasat, M. S. Gaya, I. Alav, M. A. Webber and J. M. Blair, Molecular mechanisms of antibiotic resistance revisited, *Nat. Rev. Microbiol.*, 2023, **21**, 280–295.
6 S. Gupta, N. Laskar and D. E. Kadouri, Evaluating the effect of oxygen concentrations on antibiotic sensitivity, growth, and biofilm formation of human pathogens, *Microbiol. Insights*, 2016, **9**, 37–46.
7 Y. Liang, M. Li, Y. Yang, L. Qiao, H. Xu and B. Guo, pH/glucose dual responsive metformin release hydrogel dressings with adhesion and self-healing via dual-dynamic bonding for athletic diabetic foot wound healing, *ACS Nano*, 2022, **16**, 3194–3207.
8 Y. Yang, M. Li, G. Pan, J. Chen and B. Guo, Multiple Stimuli-Responsive Nanozyme-Based Cryogels with Controlled NO Release as Self-Adaptive Wound Dressing for Infected Wound Healing, *Adv. Funct. Mater.*, 2023, 2214089.
9 F. Shafigh Kheljan, F. Sheikhzadeh Hesari, M. S. Aminifazl, M. Skurnik, S. Gholadze and G. Zarrini, Design of Phage-Cocktail-Containing Hydrogel for the Treatment of Pseudomonas aeruginosa-Infected Wounds, *Viruses*, 2023, **15**, 803.
10 A. Ali, J. Botha and R. Tiruvoipati, Fatal skin and soft tissue infection of multidrug resistant Acinetobacter baumannii: A case report, *Int. J. Surg. Case Rep.*, 2014, **5**, 532–536.
11 D. V. Zurawski, J. Banerjee, Y. A. Alamneh, J. P. Shearer and S. T. Demons, Skin and soft tissue models for Acinetobacter baumannii infection, *Acinetobacter baumannii*, Springer, 2019, pp. 271–287.
12 C. Garzoni, S. Emonet, L. Legout, R. Benedict, P. Hoffmeyer, L. Bernard and J. Garbino, Atypical infections in tsunami survivors, *Emerging Infect. Dis.*, 2005, **11**, 1591.
13 P. J. Sebeny, M. S. Riddle and K. Petersen, Acinetobacter baumannii skin and soft-tissue infection associated with war trauma, *Clin. Infect. Dis.*, 2008, **47**, 444–449.
14 N. A. Be, J. E. Allen, T. S. Brown, S. N. Gardner, K. S. McLoughlin, J. A. Forsberg, B. C. Kirkup, B. A. Chromy, P. A. Luciw and E. A. Elster, Microbial profiling of combat wound infection through detection microarray and next-generation sequencing, *J. Clin. Microbiol.*, 2014, **52**, 2583–2594.
15 C. Brives and J. Pourraz, Phage therapy as a potential solution in the fight against AMR: obstacles and possible futures, *Palgrave Commun.*, 2020, **6**, 1–11.
16 A. Zyman, A. Górski and R. Międzybrodzki, Phage therapy of wound-associated infections, *Folia Microbiol.*, 2022, 1–9.
17 F. Oechslin, Resistance development to bacteriophages occurring during bacteriophage therapy, *Viruses*, 2018, **10**, 351.
18 J. E. Egido, A. R. Costa, C. Aparicio-Maldonado, P.-J. Haas and S. J. Brouns, Mechanisms and clinical importance of bacteriophage resistance, *FEMS Microbiol. Rev.*, 2022, **46**, fuab048.
19 P. Hyman and S. T. Abedon, Bacteriophage host range and bacterial resistance, *Adv. Appl. Microbiol.*, 2010, **70**, 217–248.
20 J. Lin, F. Du, M. Long and P. Li, Limitations of phage therapy and corresponding optimization strategies: a review, *Molecules*, 2022, **27**, 1857.
21 F. L. G. Altamirano, X. Kostoulias, D. Subedi, D. Korneev, A. Y. Peleg and J. J. Barr, Phage-antibiotic combination is a superior treatment against Acinetobacter baumannii in a preclinical study, *EBioMedicine*, 2022, **80**, 104045.

22 M. Łusiak-Szelachowska, R. Międzybrodzki, Z. Drulis-Kawa, K. Cater, P. Knežević, C. Winogradow, K. Amaro, E. Jończyk-Matysiak, B. Weber-Dąbrowska and J. Rękas, Bacteriophages and antibiotic interactions in clinical practice: what we have learned so far, *J. Biomed. Sci.*, 2022, **29**, 1–17.

23 S. A. Sarker, S. Sultana, G. Reuteler, D. Moine, P. Descombes, F. Charton, G. Bourdin, S. McCallin, C. Ngom-Bru and T. Neville, Oral phage therapy of acute bacterial diarrhea with two coliphage preparations: a randomized trial in children from Bangladesh, *EBioMedicine*, 2016, **4**, 124–137.

24 P. Jault, T. Leclerc, S. Jennes, J. P. Pirnay, Y.-A. Que, G. Resch, A. F. Rousseau, F. Ravat, H. Carsin and R. Le Floch, Efficacy and tolerability of a cocktail of bacteriophages to treat burn wounds infected by Pseudomonas aeruginosa (PhagoBurn): a randomised, controlled, double-blind phase 1/2 trial, *Lancet Infect. Dis.*, 2019, **19**, 35–45.

25 M. Bahram, N. Mohseni and M. Moghtader, An introduction to hydrogels and some recent applications, *Emerging concepts in analysis and applications of hydrogels*, IntechOpen, 2016.

26 H. Y. Kim, R. Y. K. Chang, S. Morales and H.-K. Chan, Bacteriophage-delivering hydrogels: Current progress in combating antibiotic resistant bacterial infection, *Antibiotics*, 2021, **10**, 130.

27 W. Yan, P. Banerjee, Y. Liu, Z. Mi, C. Bai, H. Hu, K. K. To, H. T. Duong and S. S. Leung, Development of thermosensitive hydrogel wound dressing containing Acinetobacter baumannii phage against wound infections, *Int. J. Pharm.*, 2021, **602**, 120508.

28 C. Johnson, N. Dinjaski, M. A. Prieto and A. J. Garcia, Controlled bacteriophage release from poly(ethylene glycol) hydrogels significantly reduces infection in a bone implant-associated infection model, Front. Bioeng. Biotechnol. Conference 10th World Biomaterials Congress, 2016.

29 T. Ferry, C. Batailler, C. Petitjean, J. Chateau, C. Fevre, E. Forestier, S. Brosset, G. Leboucher, C. Kolenda and F. Laurent, The potential innovative use of bacteriophages within the DAC® hydrogel to treat patients with knee megaprosthesis infection requiring "debridement antibiotics and implant retention" and soft tissue coverage as salvage therapy, *Front. Med.*, 2020, **7**, 342.

30 K. Yang, Q. Han, B. Chen, Y. Zheng, K. Zhang, Q. Li and J. Wang, Antimicrobial hydrogels: promising materials for medical application, *Int. J. Nanomed.*, 2018, 2217–2263.

31 Y. Liang, Z. Li, Y. Huang, R. Yu and B. Guo, Dual-dynamic-bond cross-linked antibacterial adhesive hydrogel sealants with on-demand removability for post-wound-closure and infected wound healing, *ACS Nano*, 2021, **15**, 7078–7093.

32 P. Kaur, V. S. Gondil and S. Chhibber, A novel wound dressing consisting of PVA-SA hybrid hydrogel membrane for topical delivery of bacteriophages and antibiotics, *Int. J. Pharm.*, 2019, **572**, 118779.

33 J. Xiang, L. Shen and Y. Hong, Status and future scope of hydrogels in wound healing: Synthesis, materials and evaluation, *Eur. Polym. J.*, 2020, **130**, 109609.

34 S. Tavakoli and A. S. Klar, Advanced hydrogels as wound dressings, *Biomolecules*, 2020, **10**, 1169.

35 S. Nie, W. W. Hsiao, W. Pan and Z. Yang, Thermoreversible Pluronic® F127-based hydrogel containing liposomes for the controlled delivery of paclitaxel: in vitro drug release, cell cytotoxicity, and uptake studies, *Int. J. Nanomed.*, 2011, 151–166.

36 J. B. da Silva, M. T. Cook and M. L. Bruschi, Thermoresponsive systems composed of poloxamer 407 and HPMC or NaCMC: Mechanical, rheological and sol-gel transition analysis, *Carbohydr. Polym.*, 2020, **240**, 116268.

37 S. Lin, L. Pei, W. Zhang, G. Shu, J. Lin, H. Li, F. Xu, H. Tang, G. Peng and L. Zhao, Chitosan-poloxamer-based thermosensitive hydrogels containing zinc gluconate/recombinant human epidermal growth factor benefit for antibacterial and wound healing, *Mater. Sci. Eng., C*, 2021, **130**, 112450.

38 J. Chen, R. Zhou, L. Li, B. Li, X. Zhang and J. Su, Mechanical, rheological and release behaviors of a poloxamer 407/poloxamer 188/carbopol 940 thermosensitive composite hydrogel, *Molecules*, 2013, **18**, 12415–12425.

39 S. Mukhopadhyay, P. Zhang, K. K. W. To, Y. Liu, C. Bai and S. S. Y. Leung, Sequential treatment effects on phage-antibiotic synergistic (PAS) application against multidrug-resistant Acinetobacter baumannii, *Int. J. Antimicrob. Agents*, 2023, 106951.

40 F. Peng, Z. Mi, Y. Huang, X. Yuan, W. Niu, Y. Wang, Y. Hua, H. Fan, C. Bai and Y. Tong, Characterization, sequencing and comparative genomic analysis of vB_AbaM-IME-AB2, a novel lytic bacteriophage that infects multidrug-resistant Acinetobacter baumannii clinical isolates, *BMC Microbiol.*, 2014, **14**, 1–14.

41 E. M. Adriaenssens, S. M. Lehman, K. Vandersteegen, D. Vandenheuvel, D. L. Philippe, A. Cornelissen, M. R. Clokie, A. J. García, M. De Proft and M. Maes, CIM® monolithic anion-exchange chromatography as a useful alternative to CsCl gradient purification of bacteriophage particles, *Virology*, 2012, **434**, 265–270.

42 W. Bierman, The temperature of the skin surface, *J. Am. Med. Assoc.*, 1936, **106**, 1158–1162.

43 B. Leung, P. Dharmaratne, W. Yan, B. C. Chan, C. B. Lau, K.-P. Fung, M. Ip and S. S. Leung, Development of thermosensitive hydrogel containing methylene blue for topical antimicrobial photodynamic therapy, *J. Photochem. Photobiol., B*, 2020, **203**, 111776.

44 L. Bai, Z. Ma, G. Yang, J. Yang and J. Cheng, A simple HPLC method for the separation of colistimethate sodium and colistin sulphate, *J. Chromatogr. Sep. Tech.*, 2011, **2**, 1000105.

45 D. R. Alves, S. P. Booth, P. Scavone, P. Schellenberger, J. Salvage, C. Dedi, N.-T. Thet, A. T. A. Jenkins, R. Waters and K. W. Ng, Development of a high-throughput ex-vivo burn wound model using porcine skin, and its application

to evaluate new approaches to control wound infection, *Front. Cell. Infect. Microbiol.*, 2018, **8**, 196.

46 J. B. da Silva, R. S. Dos Santos, M. B. da Silva, G. Braga, M. T. Cook and M. L. Bruschi, Interaction between mucoadhesive cellulose derivatives and Pluronic F127: Investigation on the micelle structure and mucoadhesive performance, *Mater. Sci. Eng., C*, 2021, **119**, 111643.

47 S. D. Desai and J. Blanchard, In vitro evaluation of pluronic F127-based controlled-release ocular delivery systems for pilocarpine, *J. Pharm. Sci.*, 1998, **87**, 226–230.

48 A. M. Pragatheeswaran and S. B. Chen, The influence of poly(acrylic acid) on micellization and gelation characteristics of aqueous Pluronic F127 copolymer system, *Colloid Polym. Sci.*, 2016, **294**, 107–117.

49 X. Yang, Q. Qiu, G. Liu, H. Ren, X. Wang, J. F. Lovell and Y. Zhang, Traceless antibiotic-crosslinked micelles for rapid clearance of intracellular bacteria, *J. Controlled Release*, 2022, **341**, 329–340.

50 R. Y. K. Chang, Y. Okamoto, S. Morales, E. Kutter and H.-K. Chan, Hydrogel formulations containing non-ionic polymers for topical delivery of bacteriophages, *Int. J. Pharm.*, 2021, **605**, 120850.

51 S. Kumari, K. Harjai and S. Chhibber, Bacteriophage versus antimicrobial agents for the treatment of murine burn wound infection caused by Klebsiella pneumoniae B5055, *J. Med. Microbiol.*, 2011, **60**, 205–210.

52 S. Kaur, K. Harjai and S. Chhibber, Bacteriophage mediated killing of Staphylococcus aureus in vitro on orthopaedic K wires in presence of linezolid prevents implant colonization, *PLoS One*, 2014, **9**, e90411.

53 C. Attinger and R. Wolcott, Clinically addressing biofilm in chronic wounds, *Adv. Wound Care*, 2012, **1**, 127–132.

54 L. Le, M. Baer, P. Briggs, N. Bullock, W. Cole, D. DiMarco, R. Hamil, K. Harrell, M. Kasper and W. Li, Diagnostic accuracy of point-of-care fluorescence imaging for the detection of bacterial burden in wounds: results from the 350-patient fluorescence imaging assessment and guidance trial, *Adv. Wound Care*, 2021, **10**, 123–136.

55 C. Zimmermann, D. Troeltzsch, V. Gimenez-Rivera, S. Galli, M. Metz, M. Maurer and F. Siebenhaar, Mast cells are critical for controlling the bacterial burden and the healing of infected wounds, *Proc. Natl. Acad. Sci. U. S. A.*, 2019, **116**, 20500–20504.

56 E. Brambilla, S. Locarno, S. Gallo, F. Orsini, C. Pini, M. Farronato, D. V. Thomaz, C. Lenardi, M. Piazzoni and G. Tartaglia, Poloxamer-based hydrogel as drug delivery system: How polymeric excipients influence the chemical-physical properties, *Polymers*, 2022, **14**, 3624.

57 M. A. Abou-Shamat, J. Calvo-Castro, J. L. Stair and M. T. Cook, Modifying the properties of thermogelling poloxamer 407 solutions through covalent modification and the use of polymer additives, *Macromol. Chem. Phys.*, 2019, **220**, 1900173.

58 G. Baek and C. Kim, Rheological properties of Carbopol containing nanoparticles, *J. Rheol.*, 2011, **55**, 313–330.

59 I. M. Diniz, C. Chen, X. Xu, S. Ansari, H. H. Zadeh, M. M. Marques, S. Shi and A. Moshaverinia, Pluronic F-127 hydrogel as a promising scaffold for encapsulation of dental-derived mesenchymal stem cells, *J. Mater. Sci.: Mater. Med.*, 2015, **26**, 1–10.

60 S. T. Abedon, Phage-antibiotic combination treatments: antagonistic impacts of antibiotics on the pharmacodynamics of phage therapy?, *Antibiotics*, 2019, **8**, 182.

61 D. Ma, L. Li, K. Han, L. Wang, Y. Cao, Y. Zhou, H. Chen and X. Wang, The antagonistic interactions between a polyvalent phage SaP7 and β-lactam antibiotics on combined therapies, *Vet. Microbiol.*, 2022, **266**, 109332.

62 S. Moshayedi, H. Sarpoolaky and A. Khavandi, In Vitro Release Kinetics of Curcumin From Thermosensitive Gelatin-Chitosan Hydrogels Containing Zinc Oxide Nanoparticles, *Iran. J. Mater. Sci. Eng.*, 2022, **19**, 1–10.

63 A.-M. Craciun, M. L. Barhalescu, M. Agop and L. Ochiuz, Theoretical modeling of long-time drug release from nitrosalicyl-imine-chitosan hydrogels through multifractal logistic type laws, *Comput. Math. Methods Med.*, 2019, **2019**, 4091464.

64 A. Gedefie, W. Demsis, M. Ashagrie, Y. Kassa, M. Tesfaye, M. Tilahun, H. Bisetegn and Z. Sahle, Acinetobacter baumannii biofilm formation and its role in disease pathogenesis: a review, *Infect. Drug Resist.*, 2021, 3711–3719.

65 J. A. Wroe, C. T. Johnson and A. J. García, Bacteriophage delivering hydrogels reduce biofilm formation in vitro and infection in vivo, *J. Biomed. Mater. Res., Part A*, 2020, **108**, 39–49.

66 W. Fu, T. Forster, O. Mayer, J. J. Curtin, S. M. Lehman and R. M. Donlan, Bacteriophage cocktail for the prevention of biofilm formation by Pseudomonas aeruginosa on catheters in an in vitro model system, *Antimicrob. Agents Chemother.*, 2010, **54**, 397–404.

67 O. Ciofu, C. Moser, P. Ø. Jensen and N. Høiby, Tolerance and resistance of microbial biofilms, *Nat. Rev. Microbiol.*, 2022, **20**, 621–635.

68 X. Chen, M. Liu, P. Zhang, M. Xu, W. Yuan, L. Bian, Y. Liu, J. Xia and S. S. Leung, Phage-derived depolymerase as an antibiotic adjuvant against multidrug-resistant Acinetobacter baumannii, *Front. Microbiol.*, 2022, **13**, 845500.